A Mesoporous Silica Biomaterial for Dental Biomimetic Crystallization

Yu-Chih Chiang,[†,⊥] Hong-Ping Lin,[§,⊥] Hao-Hueng Chang,[†] Ya-Wen Cheng,[†] Hsin-Yen Tang,[†] Wei-Ching Yen,[†] Po-Yen Lin,[‡] Kei-Wen Chang,[§] and Chun-Pin Lin*[,†]

[†]School of Dentistry and Graduate Institute of Clinical Dentistry, National Taiwan University and National Taiwan University Hospital, No. 1, Chang-Te Street, Taipei 10016, Taiwan, [‡]Department of Dentistry, School of Dentistry, National Yang-Ming University, No. 155, Sec. 2, Linong Street, Taipei, 112 Taiwan, and [§]Department of Chemistry, National Cheng Kung University, No. 1, Daxue Road, Tainan City, 701, Taiwan. [⊥]Yu-Chih Chiang and Hong-Ping Lin contributed equally.

ABSTRACT The loss of overlying enamel or cementum exposes dentinal tubules and increases the risk of several dental diseases, such as dentin hypersensitivity (causing sharp pain and anxiety), caries, and pulp inflammation. This paper presents a fast-reacting, more reliable and biocompatible biomaterial that effectively occludes exposed dentinal tubules by forming a biomimetic crystalline dentin barrier. To generate this biomaterial, a gelatin-templated mesoporous silica biomaterial ($CaCO_3$@mesoporous silica, CCMS) containing nanosized calcium carbonate particles is mixed with 30% H_3PO_4 at a 1/1 molar ratio of Ca/P (denoted as CCMS-HP), which enables Ca^{2+} and PO_4^{3-}/HPO_4^{2-} ions to permeate the dentinal tubules and form dicalcium phosphate dihydrate (DCPD), tricalcium phosphate (TCP) or hydroxyapatite (HAp) crystals at a depth of approximately 40 μm (sub-μ-CT and nano-SEM/EDS examinations). *In vitro* biocompatibility tests (WST-1 and lactate dehydrogenase) and ALP assays show high cell viability and mineralization ability in a transwell dentin disc model treated with CCMS-HP ($p < 0.05$). The *in vivo* efficacy and biocompatibility analyses of the biomaterial in an animal model reveal significant crystal growth (DCPD, TCP or HAp-like) and no pulp irritation after 70 days ($p < 0.05$). The developed CCMS-HP holds great promise for treating exposed dentin by growing biomimetic crystals within dentinal tubules. These findings demonstrate that the mesoporous silica biomaterials presented here have great potential for serving as both a catalyst and carrier in the repair or regeneration of dental hard tissue.

KEYWORDS: biomimetics · crystal growth · dentinal tubule · mesoporous materials · sub-μ-CT

Dentin has a tubular structure, which is normally protected by the overlying enamel (crown) or cementum (root), and is the major component of human teeth and protects the pulp tissue. When either the overlying enamel or cementum is breached dentin is exposed to the oral environment in which the exposed dentinal tubules provide channels for the permeation of solutes, irritants, and bacteria. Consequently, several aggravating symptoms or related diseases result from exposed dentinal tubules.[1,2] For instance, in the case of vital tooth, once the fluid flow within the dentinal tubules is changed by air-flow, evaporation, or thermal, tactile, osmotic, or chemical stimuli, movement of the fluid will cause deformation of the nerve endings at the Raschkow plexus, leading to stimuli transmission and thereby causing dentin hypersensitivity.[3,4] Dentin hypersensitivity, defined as a short, sharp pain resulting from exposed dentinal tubules, is one of the most troublesome and common complaints expressed by patients.[5,6] Several hypothesis have been proposed over the past century to explain the mechanism of dentin hypersensitivity. Among which, the hydrodynamic theory proposed by Brannstrom is currently the most widely accepted one.[3] This hypothesized mechanism requires not only the dentinal tubules must be exposed to the oral environment, but the tubules have to be open at the dentin surface. Indeed, sensitive teeth have greater numbers of open tubules (8×) and wider (2×) tubules at the buccal cervical area compared with nonsensitive teeth.[7] The resultant alterations in dentinal fluid flow and pulpal hemodynamics may cause variations in dentin hypersensitivity over time. Additionally, the increased number and width of patent dentinal tubules may increase the severity of dentin hypersensitivity.[8] The pain

* Address correspondence to pinlin@ntu.edu.tw.

Received for review September 21, 2014 and accepted December 7, 2014.

Published online December 08, 2014
10.1021/nn5053487

induced by external stimuli is consistent with the grade of dentin hypersensitivity, which also induces anxiety and increases corticosterone levels in serum.[2] Thus, occluding exposed dentinal tubules is a crucial strategy for preventing irritants invasion, reducing dentinal tubule permeability, and, subsequently, preventing the progression of related dental diseases.[9−11]

Over the decades, a large number of desensitizing agents that aim at occluding dentinal tubules have been commercially available. But so far, none of them are accepted as a consistent and reliable treatment regimen. Potassium oxalate, for example, has been recommended as an effective treatment for dentin hypersensitivity decades ago.[12] But the consequently formed calcium oxalate crystal was found to dissolve when immersed in artificial saliva,[13] which made clinical treatment outcome rather short-lived. Sodium fluoride was also frequently used as desensitizing agent. It is believed that calcium fluoride crystals would form on the surface of dentinal tubules. But the large calcium fluoride crystals only cover the surface of the exposed dentin, which can be easily removed.[14,15] Recently, a number of commercial dental care products for daily use (such as Sensodyne Prophylaxis Paste with NovaMin and Colgate Sensitive Pro-Relief Toothpaste) were developed to occlude exposed dentinal tubules.[16−18] Unfortunately, the precipitates from these commercial products only penetrate into the dentinal tubules approximately 2−10 μm, which may not combat the daily adverse conditions in the oral environment, such as erosion and tooth wear, resulting from chewing, brushing, and mechanical force. If the precipitates do not penetrate into the dentinal tubules deep enough, they would soon be worn out.[19,20]

Therefore, it is preferable to develop biomaterials for more effective biomimetic barriers that can precipitate deeper into the dentinal tubules without irritating the pulp, rapid in action, and provide lasting tubule occlusion in dentin.[4] Since the main components of dentin are calcium phosphates, it is biomimetic that the dentinal tubules be occluded with the similar mineral compound. However, effective occlusion is difficult to achieve due to the complex nature of the pulp-dentin structure. In addition to the effect of the outward hydraulic pressure (0.15 kg/cm^2) produced by dental pulp, it is difficult to precipitate material inside the tubules within a short time and at long depths because of the tiny dimensions (0.5−4 μm in diameter) of hydrolytic dentinal tubules and a protein-like membrane, the *lamina limitans*.[21] Thus, developing a method to form calcium phosphate (Ca−P) or hydroxyapatite (HAp)-like crystalline precipitates within dentinal tubules would provide a consistent and biocompatible means for filling these structures.[22−24] Ca−P materials are of special interest in oral biology and medicine because of (a) their occurrence in normal apatite, which occurs as $(Ca, Z)_{10}(PO_4, Y)_6(OH, X)_2$ (Z = Na, Mg, K, Sr; Y = CO_3, HPO_4; X = Cl, F) in enamel, dentin, cementum, and bone; (b) their roles in the initiation, progression, and arrest of caries; and (c) their use in tissue engineering applications. Imai and Akimoto using 5% of disodium phosphate solution followed by rubbing with 10% calcium chloride solution on dentin surface. Rapid precipitation of calcium phosphate was found at the surface of dentin, but did not penetrate into the dentinal tubules to produce sustained occlusion.[25] Ishikawa *et al.* demonstrated that an acidic solution containing Ca^{2+} and HPO_4^{2-} prevents rapid precipitation on dentin surface from blocking the openings of dentinal tubules in which the precipitate may occlude the exposed dentinal tubules to a depth of 4−10 μm.[26] However, this shallow precipitate does not guarantee a positive clinical outcome. Our previous studies have shown that DP-bioglass mixed with 30% phosphoric acid can occlude dentinal tubules to a depth of 60 μm[27,28] and exhibits high biocompatibility.[29] Despite these positive results, the long reaction time (3 days) and low occlusion percentage limit the use of DP-bioglass and compromise the desired clinical outcome.

In crystallography, the supersaturation of solutions plays a vital role in the precipitation of crystallites and may be used to overcome the challenges associated with the permeation of ions into the tiny dentinal tubules. Mesoporous silicas possess well-defined structures, high surface areas, tunable pore sizes, hydrocarbon sorption efficacy, and high thermal/hydrothermal stability; as such, mesoporous silicas have been widely researched over the past two decades.[30−32] Because of their unique characteristics, these materials are well suited for use as catalysts or supports in sorption and separation processes, electronic and optical materials, and catalytic reactions.[33,34] For this reason, we employed mesoporous silica foams as a carrier for nano-CaO particles (nano CaO@mesoporous silica, NCMS). The NCMS was synthesized from an emulsion of toluene and the triblock copolymer Pluronic P123 ($EO_{20}−PO_{70}−EO_{20}$). When the NCMS was mixed with an appropriate amount of phosphoric acid, the paste released significant amounts of calcium ions and hydrogen phosphate (HPO_4^{2-}) species, which react with teeth.[35] The formed $CaHPO_4 \cdot 2H_2O$ (denoted as DCPD) crystals can achieve a depth of approximately 100 μm,[35] which tightly occludes the dentinal tubules. However, the slow dissolution of CaO requires more phosphoric acid to promote the penetration of ions into the tubules. In addition, the synthesis of the NCMS requires the use of Pluronic P123 and toluene, the latter of which is a neuro-toxin and irritates the skin and mucosa. Furthermore, reacting toluene with oxygen produces benzaldehyde and cresol, which contribute to pollution.

Herein, we report a biocompatible Ca−P biomaterial that contains a mixture of $CaCO_3$@mesoporous silica

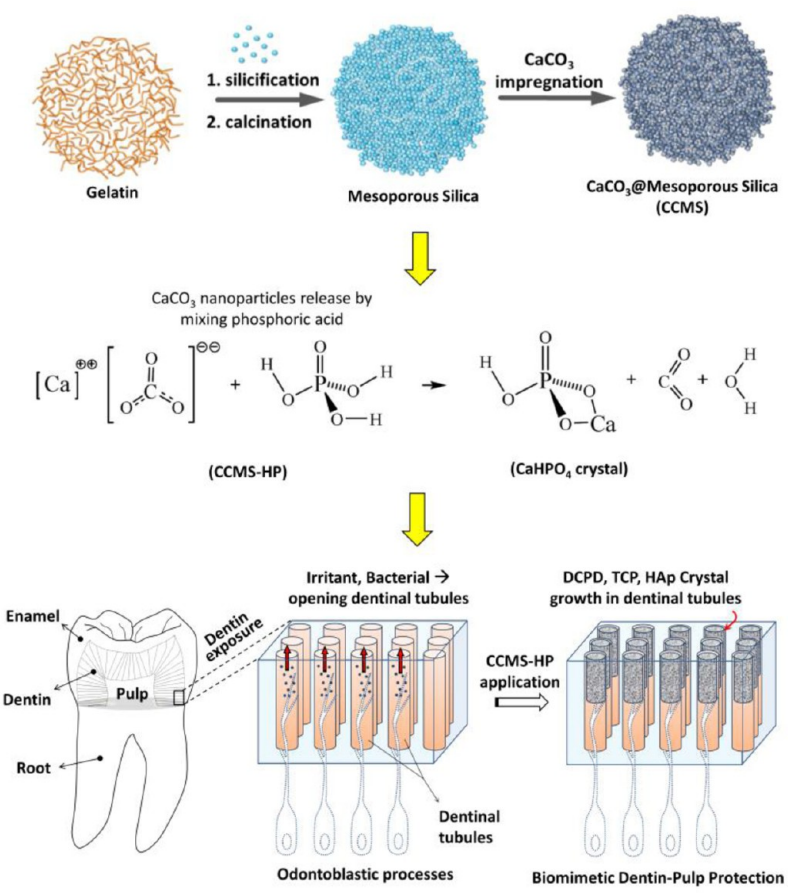

Scheme 1. Synthetic route for preparing $CaCO_3$@mesoporous silicate (CCMS) and a schematic illustration of the application and mechanism of CCMS-HP (CCMS mixed with phosphoric acid) on the exposed dentin surface for the biomimetic protection of the dentin–pulp complex through DCPD, TCP or HAp-like crystal growth in dentinal tubules.

(CCMS) in which the mesoporous silica is templated using biocompatible gelatin. The mesoporous silica would act as a carrier and reservoir to supply calcium ions. The addition of an appropriate amount of phosphoric acid to form the CCMS-HP paste almost completely occludes dentinal tubules within 10 min through the formation of an intact biomimetic Ca–P protective barrier at the surface of the tubules. Because of the lattice matching of the DCPD- or HA-like precipitates, rapid occlusion of the dentin tubules proceeds *via* a heterogeneous-nucleation mechanism rather than *via* a homogeneous-nucleation mechanism with higher activation energy. The preparation procedure and occlusion mechanism of the CCMS-HP paste are summarized in Scheme 1. The efficacy of dentinal tubule occlusion, crystal characterization, biocompatibility, and dental pulp irritation were evaluated *in vitro* and *in vivo*.

RESULTS AND DISCUSSION

Optimization and Characterization of $CaCO_3$@Mesoporous Silica/H_3PO_4 (CCMS-HP). To determine the optimal ratio of CCMS to 30% H_3PO_4 (denoted as CCMS-HP) for the paste, we prepared pastes with various ratios to measure their pH values and permeation depths in dentinal tubules (Table 1). The optimization of the CCMS-HP ratio was based on minimizing erosion while achieving effective ion permeation in the dentinal tubules. The optimal ratio of CCMS-HP was a Ca/P molar ratio = 1/1. Nondestructive ultrahigh resolution (500 nm^3/voxel) Sub-Micron X-ray Computed Tomography (Sub-μ-CT) indicated that the percentage of successfully occluded tubule openings reached nearly 100% after treatment with CCMS-HP paste for 5 min (Figure 1 and Supporting Information, Video S1). The crystals grew within the dentinal tubules to a depth of approximately 40–60 μm. The higher density of the crystalline column within the tubules may form a protective barrier against chewing forces or bacterial invasion (Figure 1c). Furthermore, the pH of the CCMS-HP paste (Ca/P molar ratio = 1/1), which was found to be between 5.3 and 6.5, did not cause any significant dentin erosion. The critical pH value for the erosion of dentin is normally approximately 6.0–6.8.[36] Featherstone *et al.* proposed that dentin would not be eroded if exposed to supersaturated Ca^{2+} and PO_4^{3-} ions, even at pH values lower than the critical pH value.[37] CCMS provides a similar environment when mixed

TABLE 1. Effects of Various Ratios of CCMS Powder and 30% H_3PO_4 Liquid on the pH Value and Permeation Depth of Crystallization in Dentinal Tubules (n = 6)

Ca/P molar ratio	1/4	1/3	1/2	1/1	2/1
resulting pH value	2.8−3.2	3.5−4.7	4.4−5.4	5.3−6.5	6.2−7.0
crystal growth depth [μm] (mean ± SD)*	101.7 ± 10.4[a]	69.4 ± 10.8[b]	65.4 ± 11.7[b]	39.8 ± 9.1[c]	1.4 ± 1.1[d]

* The same superscript letter indicates that there were no significant differences ($p > 0.05$).

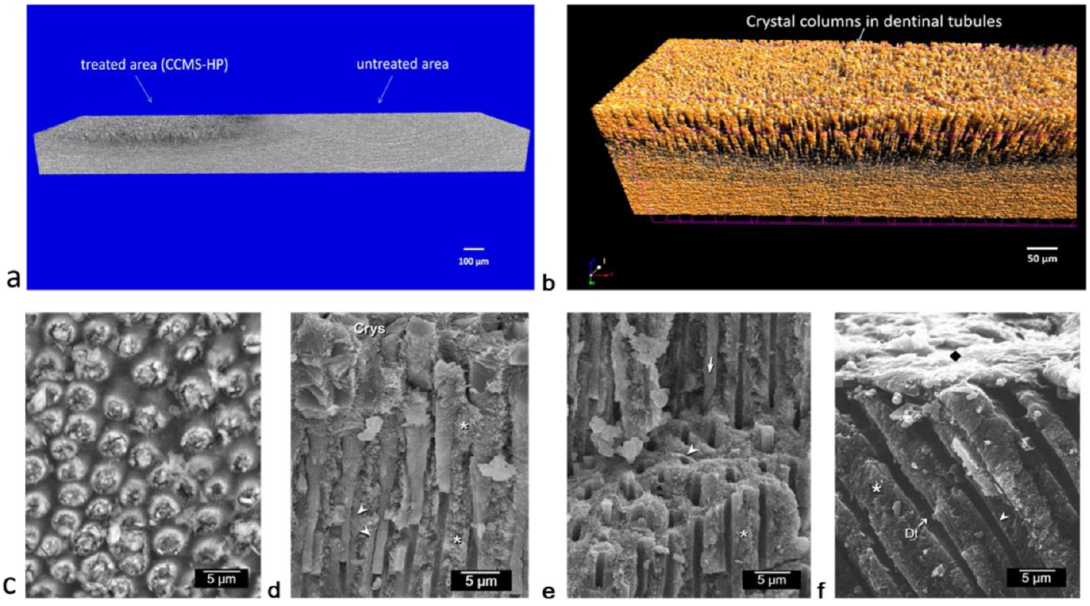

Figure 1. Crystallization in dentinal tubules treated using CCMS-HP with a Ca/P molar ratio of 1/1 (the *in vitro* efficacy of biomimetic occlusion): (a) 3D image reconstruction of the μCT data set. (b) ROI of the 3D image shows the crystal columns in dentinal tubules. (c) Cross-sectional surface of a dentin disc after the application of CCMS-HP. The dentinal tubules were completely occluded with CCMS-HP precipitates. (d) A superficial part and (e) a deeper section of split dentin revealed the precipitates within dentinal tubules by treatment with CCMS-HP. Peritubular (arrowhead) and intertubular dentin (asterisk) are observed along the crystals. (Crys, crystallization on dentin surface). (f) CCMS-HP (Ca/P molar ratio = 0.5/1) of the pH 6.0−7.0 group revealed that precipitates (♦) were only observed on the dentin surface and were less in the dentinal tubules (Dt).

with phosphoric acid, immediately producing supersaturated Ca^{2+} and PO_4^{3-} ions on the dentin surface and thus preventing acid erosion of the dentin during occlusion.

The resulting 39.8 ± 9.1 μm crystalline precipitate depth in dentinal tubules showed more promising and efficient occlusion compared to current commercial products (shallow occlusion about 2−10 μm[16−18]). Considering the pH of the paste and the allowed depth for crystal growth, we chose to investigate the *in vivo* efficacy, biocompatibility, and propensity to irritate dental pulp of a CCMS-HP mixture with a determined Ca/P molar ratio of 1/1 and pH value of 5.3−6.5.

Crystallization and Characterization of CCMS-HP. We used gelatin as a template to prepare the mesoporous silica because the hydrolytes of gelatin (polypeptides) contain numerous amino groups that can produce the hydrogen functional groups required to react with sodium silicate to form mesoporous silica. When formed using this approach, the mesoporous silica contains nanopores that restrict the size of any embedded $CaCO_3$ particles. The porous ultrastructure of the CCMS particles allows them to serve as $CaCO_3$ carriers. The cloudy appearance of the material indicates the presence of nanosized $CaCO_3$ (Figure 2). An analysis of the N_2 adsorption−desorption isotherm showed that the surface area and pore size of the prepared mesoporous silica were approximately 450 $m^2\ g^{-1}$ and 7.0 nm, respectively. Consequently, the $CaCO_3$ particles of high surface-to-volume ratio loaded in the mesoporous silica quickly dissolve when in contact with phosphate-containing acidic solutions.

Figure 2b shows that when the CCMS powder was mixed with 30% H_3PO_4, 2−3-μm plate-like crystals were distributed around the mesoporous silica spheres. The number and volume of plate-like crystals increased after the continuous reaction of the CCMS-HP (Figures 2b,c and Supporting Information, Figure S1). The numerous nanopores in the CCMS provided a reservoir for absorbed phosphoric acid, which enables subsequent reaction with the embedded nanosized $CaCO_3$ particles, thereby continuously releasing Ca^{2+} and HPO_4^{2-}. In addition, the presence of silica in the supersaturated solution of Ca^{2+} and HPO_4^{2-} or PO_4^{3-} ions may promote the formation of apatite crystals, even in the presence of hydroxyapatite formation inhibitors.[38−40]

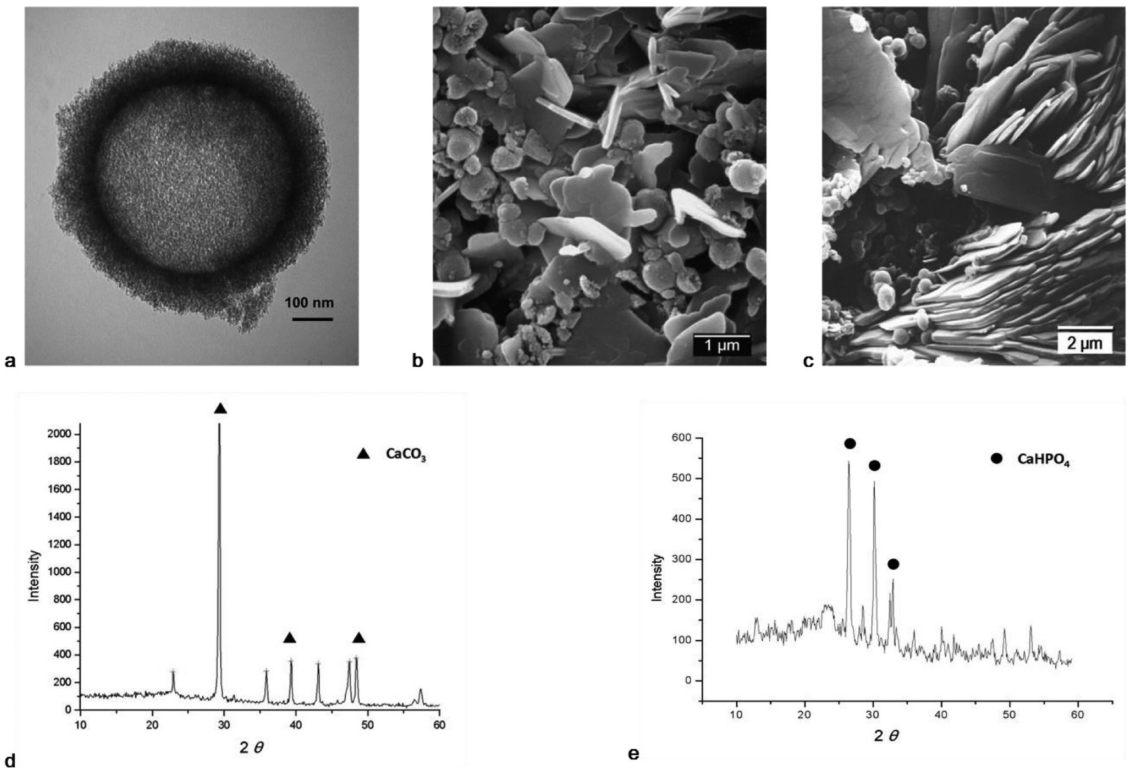

Figure 2. Characterization of mesoporous silica and CCMS-HP (Ca/P molar ratio = 1/1). (a) TEM image of mesoporous silica particle (CCMS powder) with nanopores that serve as a $CaCO_3$ carrier. (b) and (c) show CCMS-HP after aging times of 1.0 and 3.0 min. The $CaHPO_4$ crystallized on the mesoporous silica spheres. As the aging time increases, more $CaHPO_4$ grows into plate-like and bulk crystals. X-ray diffraction patterns of the (d) CCMS powder and (e) CCMS-HP crystalline product indicated that the main components are $CaCO_3$ (▲) and $CaHPO_4$ (●), respectively.

In the absence of mesoporous silica, it has been proposed that the mechanism by which supersaturated Ca^{2+} and HPO_4^{2-} ions prefer to precipitate on the dentin surface; however, their occlusion depth is shallow (5−10 μm)[26] because within the dentinal tubule, there is a lack of sufficient and continuous support for the Ca^{2+} and HPO_4^{2-} or PO_4^{3-} ions from the material. To overcome this difficulty, we used a mesoporous silica material with phosphoric acid-dissolved nanosized calcium carbonate. The supersaturation of Ca^{2+} and HPO_4^{2-} ions releasing from CCMS-HP tend to precipitate on the mesoporous silica rather than on the dentin surface (Supporting Information, Figure S1). The pore-opening dentin tubules allow the continuously penetration of the Ca^{2+} and HPO_4^{2-} ions by the concentration gradient force.

To explore the mechanism of ion permeation in dentinal tubules, we assayed the permeation of various ions using a dentin disc model (Supporting Information, Figure S3). HPO_4^{2-} and PO_4^{3-} play key roles as leading ions that recruit Ca^{2+} from the CCMS-HP. When $Ca(OH)_2$ is mixed with distilled water, no Ca^{2+} permeates through the dentin tubules; accordingly, no crystal growth occurs in the dentinal tubules. The permselective character of the dentinal tubule attracts PO_4^{3-} into its structure, allowing this ions to permeate throughout the structure. In the present study, the concentrations of PO_4^{3-} and Ca^{2+} increased with time. PO_4^{3-} permeated significantly more than Ca^{2+}, reinforcing the hypothesis that PO_4^{3-} permeates through the tubules more easily than Ca^{2+}. As a result, the PO_4^{3-} or HPO_4^{2-} concentration decreased with increasing depth, whereas the concentration of Ca^{2+} stabilized over the length of the tubules. Additionally, the calcium-phosphates ion product constant Q_{sp} (2.57×10^{-6}) surpassed the K_{sp} (2.3×10^{-7}) for the precipitation of DCPD. The PO_4^{3-}, HPO_4^{2-}, and Ca^{2+} ion concentrations would not increase above this threshold due to the formation of DCPD crystals.

XRD analysis and JCPDS mapping revealed strong diffraction peaks at 2θ = 29.4°, 48.4°, and 39.3°, indicating that the main component of the CCMS powder is $CaCO_3$ (Figure 2d). When the CCMS powder was mixed with 30% H_3PO_4, the strongest diffraction peaks appeared at 2θ = 26.4°, 30.1°, and 32.8°, suggesting that the main precipitate in this case was $CaHPO_4$ (Figure 2e). Note that crystal growth within dentinal tubules may produce crystal structures that are slightly different than those observed for the $CaHPO_4$ precipitate formed upon mixing CCMS and H_3PO_4. This difference is due to the unique structure of the dentinal lumen and the nature of the ion exchange that occurs within it, which would likely produce crystals with TCP or HAp ordering.

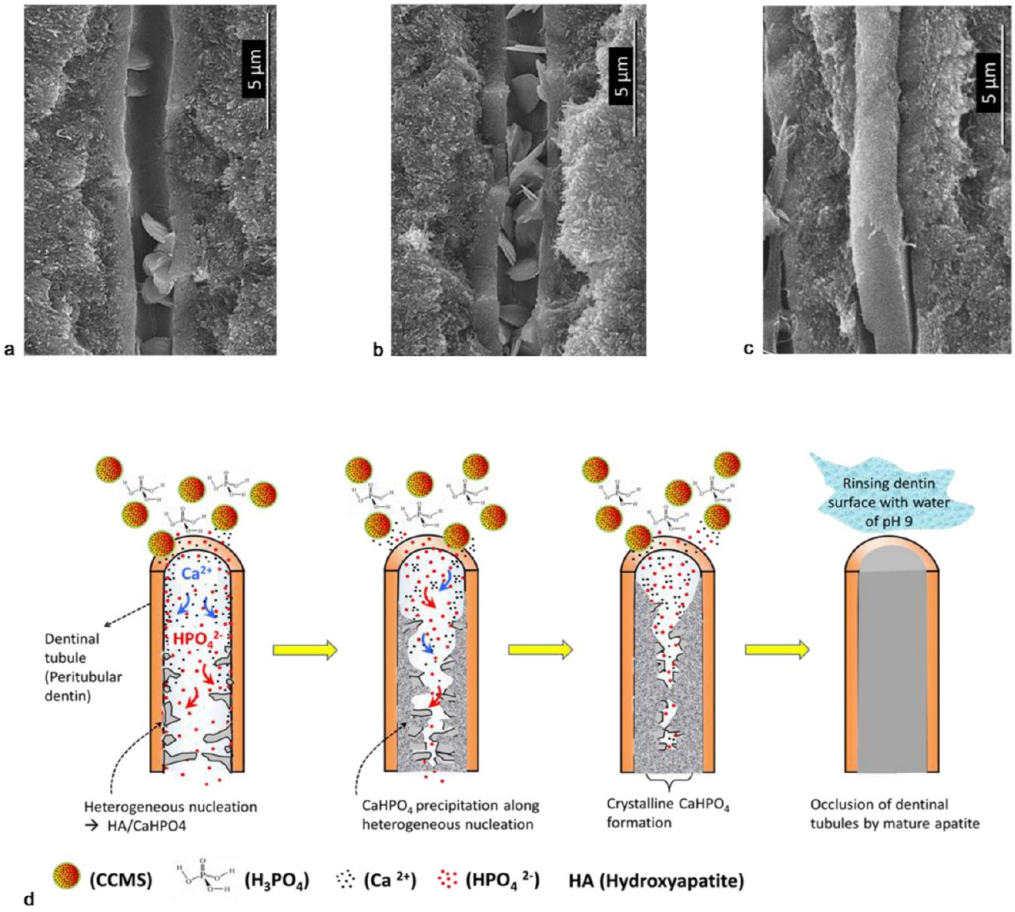

Figure 3. Mechanism for the formation of apatite calcium phosphate in dentinal tubules by treatment with CCMS-HP paste. SEM showed precipitates in dentinal tubules when the CCMS-HP paste was applied to the dentin for various durations, (a) 1 min or (b) 2 min, and then the reaction was stopped by dehydration. (c) The completion of crystallization in a dentinal tubule. (d) An illustration shows the mechanism of the crystallization process in a dentinal tubule.

Figure 3a and 3b show the initial stage of crystal growth in the dentinal tubules induced by the reaction of CCMS-HP on the dentin surface. When the CCMS-HP surface reaction was halted, a few hydroxyapatite-like or DCPD crystals formed along the tubule walls. If the CCMS-HP was allowed to continue reacting on the dentin surface (*i.e.*, the Ca^{2+} and PO_4^{3-} or HPO_4^{2-} ions continue permeating the dentinal tubules), the crystals grew and filled the dentinal tubules (Figure 3c). Figure 3d illustrates the mechanism for the formation of apatite calcium phosphate in dentinal tubules treated with the CCMS-HP paste. The favorable heterogeneous nucleation of calcium phosphates are induced along the wall of the tubules without forming a strong chemical bond to the dentin itself. This nucleation prevents the self-crystallization on the tooth surface, which would block the permeation of ions.

To determine whether the Ca^{2+} generated in the mesoporous silica contributed to the formation of precipitates in the tubule, we synthesized $SrCO_3$@mesoporous silicate and monitored the presence of Sr within the formed crystals. The $SrCO_3$@mesoporous silicate was mixed with H_3PO_4 to induce the precipitation of crystals in dentinal tubules. EDS analysis showed that Sr was the principal cationic element within the precipitate in the tubule (Supporting Information, Figure S4). Elemental mapping also indicated that Sr was present in the crystals within the tubule, along with Ca and P. These results suggest that the dentinal structure may also release Ca^{2+} ions to participate in the growth of DCPD due to the permeation of PO_4^{3-} or HPO_4^{2-}; however, the main source of Ca^{2+} ions is the CCMS-HP paste.

***In Vitro* Biocompatibility Tests.** WST-1 and LDH assays (Figures 4a and 4b) showed that the presence of CCMS-HP exhibited a high level of cell viability (100% cell proliferation and 25.4−28.7% cell lysis), as did other groups (Seal & Protect and DMEM control group), in a transwell dentin disc model with a 200-μm dentin barrier (TDD model, see Supporting Information, Figure S5). The transwell pore size was 3.0 μm, which simulates the diameter of dentinal tubules close to the pulp chamber. When tested in the elution model, WST-1 and LDH assays (Supporting Information, Figure S7) showed that the CCMS exhibited the highest cell viability (3T3 fibroblasts) of all groups over the whole culture period ($P < 0.05$). However, the cell proliferation decreased when CCMS was mixed with 30% H_3PO_4 (CCMS-HP group). Seal & Protect, a commercial product, resulted

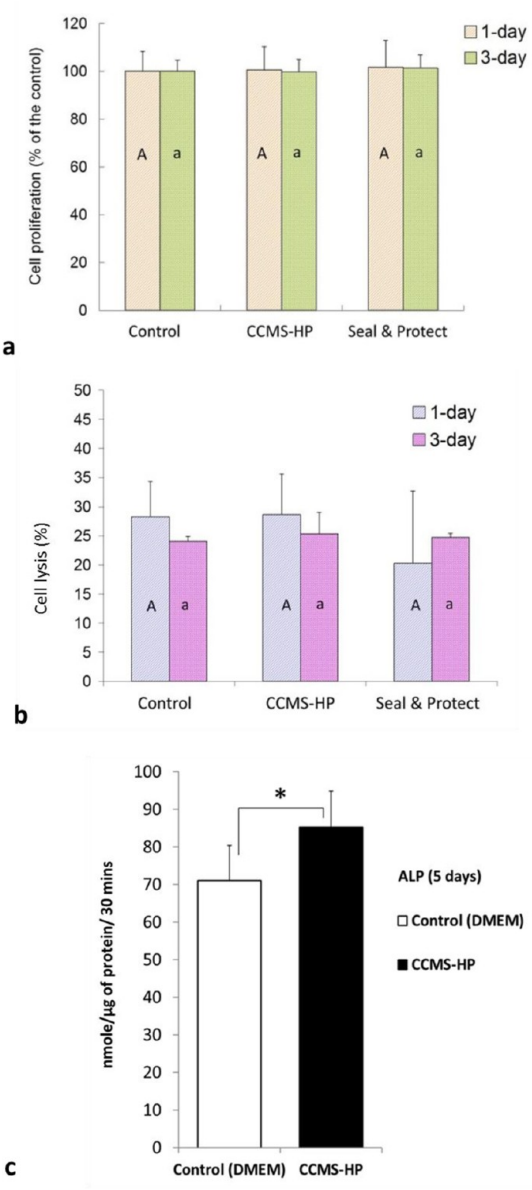

Figure 4. Effects of CCMS-HP on dental pulp cells: a biocompatibility test and ALPase activity assay (n = 6). (a) The pulp cell morphology response to CCMS-HP of the TDD model and WST-1 assay. (b) LDH assay of CCMS-HP of the TDD model. The same letter indicates that there were no significant differences ($p > 0.05$), where S&P = Seal & Protect. (c) ALPase activity assay with elution of the extract in the TDD model after 5 days. ALP activity assay was statistically analyzed using the Mann–Whitney U test. (*Statistically significant difference, p-value = 0.041). Bar = Standard deviation.

in the lowest cell viability ($P < 0.05$). The results suggested that phosphoric acid contributed to the cytotoxicity of CCMS-HP. For the clinical situations, the tooth cavity or exposed dentin normally presents a certain thickness of dentin barrier, CCMS-HP would not direct contact the dental pulp.

CCMS-HP- and DMEM-treated dental pulp cells were stained blue under light microscopy observations (ALP staining, see Supporting Information, Figure S8). The *in vitro* pulp cells appeared normal morphologies after immersion in the extract of CCMS-HP in the TDD model. The quantitative ALPase assay indicates that the elution of CCMS-HP may has the potential to induce the activity of ALPase through the dentin barrier (Figure 4c). That is, CCMS-HP takes advantage of the remineralization ability of the dental pulp cells due to the permeating Ca^{2+} ions. Ca^{2+} is a vital regulator of cell functions. For example, increased mRNA expression of osteopontin and bone morphogenetic protein BMP-2 can be induced by elevating the Ca^{2+} concentration by 0.7 mM.[41] Thus, Ca^{2+} is vital for inducing the formation of human hard tissue, and the Ca^{2+} released from the proposed mesoporous silica compound plays a role in the regulation of mineralization by pulp cells, suggesting that CCMS-HP may be useful as a pulp-capping material. Thus, in clinical applications, the exposed dentin produced by deep caries may be treated by applying CCMS-HP, which forms an integrated biomimetic protective barrier to maintain pulp vitality and promote mineralization repair.

Animal Study: Dental Pulp Irritation Tests. Figure 5a shows the sequence followed to expose dentinal tubules and the subsequent materials therapy (CCMS-HP, IRM or Seal&Protect) employed in the *in vivo* pulp irritation and efficacy tests. Figures 5b,c show representative histological analyses with mild inflammatory responses to the Seal & Protect treatment. In this case, the blood vessels were filled with erythrocytes, which indicates congestion. For the CCMS-HP-treated group (Figures 5e–g) and the IRM control group, no pulp inflammation was observed, regardless of the length of the examination period. For example, the 7-d CCMS-HP-treated group exhibited pseudostratified lining of the odontoblast layer in the pulp tissue without the infiltration of inflammatory cells (Figure 5e). Moderate pulp inflammation occurred only in the group treated with Seal & Protect, for which the blood vessels were filled with erythrocytes, and the infiltration of a significant amount of inflammatory cells indicated congestion (Figure 5d, Day 70). No severe inflammation was observed in any of the specimens. Figure 5h presents the statistical results of the *in vivo* pulp irritation tests using various test materials. No statistically significant differences were observed among the three groups in each period ($P > 0.05$). However, significant differences were observed when all specimens were combined ($P = 0.033$), and Dunn's post-test indicated a significant difference between the CCMS-HP-treated group and the group treated with Seal & Protect. Overall, the animal study revealed that the CCMS-HP paste exhibited a more favorable dentin–pulp response than did the other treatments.

Animal Study: *In Vivo* Efficacy and Characteristic Crystal Growth Evaluations. Figure 6 presents the SEM/EDS analyses of the CCMS-HP precipitates formed in an animal model. The precipitates permeated to depths of 30–50 μm in the dentinal tubules. In the *in vivo* environment

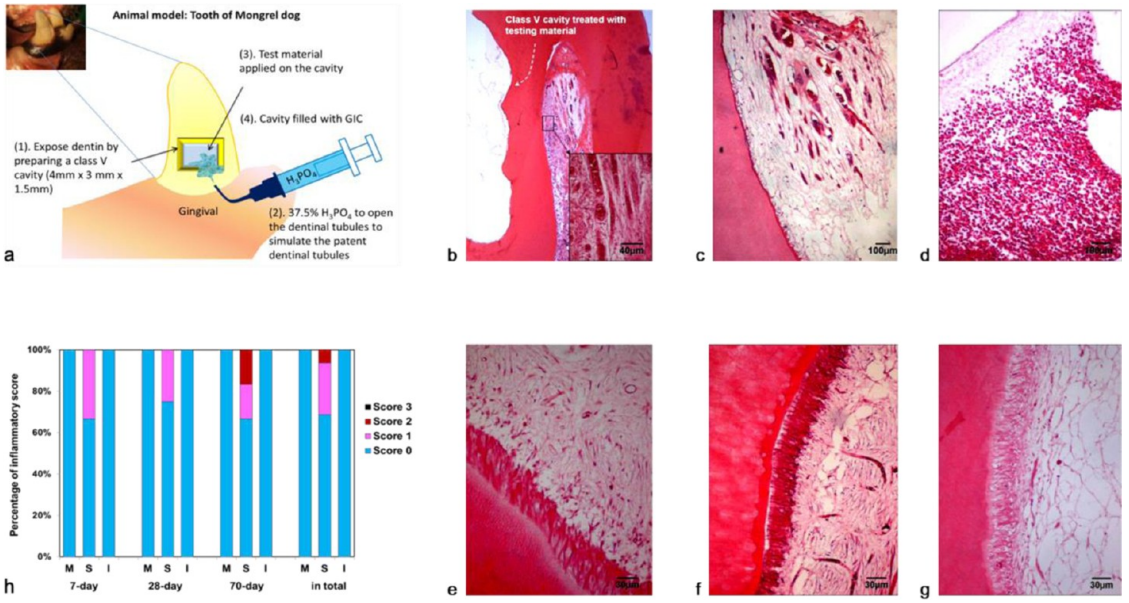

Figure 5. Pulp irritation tests and histologic analysis in an animal study (12-month-old mongrel dog). (a) Illustration of the sequence used to expose dentinal tubules. (b−h) Histological analysis (H&E stain) and scores for the pulp inflammatory response. The pulp inflammation score was categorized from "none" to "severe" (score 0 to 3) according to the criteria of Heyeraas *et al.*[42] The Seal & Protect-treated group generally presented no or mild-to-moderate inflammation: (b) 7 d, mild inflammation, lymphocytes infiltrated pulp tissue. Blood vessels were filled with erythrocytes, revealing hemorrhage conditions; (c) 28 d, mild inflammation; (d) 70 d, moderate inflammation, chronic inflammatory cells, mostly lymphocytes and plasma cells, infiltrated pulp tissue. The CCMS-HP-treated group showed no inflammation, retaining the pseudostratified appearance of the odontoblasts: (e) 7, (f) 28, and (g) 70 d. (h) Scores for pulpal inflammatory response to CCMS-HP (M), Seal & Protect (S), and IRM (I) at 7, 28, 70 d, and the total scores. CCMS-HP and IRM (negative control) exhibited no pulp inflammatory response. There were significant differences between CCMS-HP and Seal & Protect ($p < 0.05$).

presented here, in which dentin was exposed to outward pressure from dentinal fluid, the CCMS-HP crystals filled almost all of the tubules. The ultrastructures of the precipitates and dentin can easily be distinguished under higher magnification. The precipitates permeated the dentinal tubules without eroding the dentin. For the teeth treated with Seal & Protect, the surface of the dentin was covered with a thin layer of resin, which penetrated the dentinal tubules to a depth of approximately 5−10 μm. An obvious gap (10 μm) between the Seal & Protect resin and the dentin surface was observed (Figure 6d), indicating the formation of a defect that may potentially lead to future irritation and infection.

Human dentin normally exists at a hydrostatic pressure of approximately 14.1 cm·H_2O from the pulp.[43] Suge *et al.* used the method of calcium phosphate precipitation on live dog dentin and achieved crystallization to a depth of only 5 μm in the dentinal tubules (half of the depth observed in the *in vitro* dentin test in the present study).[44] The rapid precipitation of DCPD and self-crystallization of $Ca_3(PO_4)_2$ on the dentin surface blocks the permeation of ions. The chemical reaction is suggested as follows:

$$Ca^{2+} + HPO_4^{2-} + 2H_2O \rightarrow CaHPO_4 \cdot 2H_2O$$

$$2CaHPO_4 \cdot 2H_2O + Ca^{2+} \rightarrow Ca_3(PO_4)_2 + 2H^+ + 2H_2O$$

The shallow precipitates on the dentin surface can easily be washed out by tooth brushing or an acidic diet, which compromises the intended outcome of the treatment. Because of the higher hydrostatic pressure of the pulp (32.6 cm·H_2O) in live dog teeth, it is more difficult to grow crystals in dog dentinal tubules than it is in a human tooth (14.1 cm·H_2O). CCMS-HP can form crystals at depths of more than 30 μm in dog dentinal tubules *in vivo*, indicating that the CCMS-HP biomaterial has excellent potential for the long lasting occlusion of dentinal tubules.

EDS revealed that the number Ca/P of crystals formed in the tubule increased as the depth of the crystallization site increased (Figure 6). The dentinal wall is composed of nonstoichiometric calcium-deficient hydroxyapatite, $Ca_{10-x}(HPO_4)_{6-x}(OH)_{2-x}$ ($0 < x < 2$), which induces heterogeneous nucleation for the precipitation of DCPD. When the supersaturated Ca^{2+} and PO_4^{3-} or HPO_4^{2-} ions permeate deeper into the fluid of the dentinal tubules, the pH increases due to the decreasing concentrations of PO_4^{3-} and HPO_4^{2-} ions in the surrounding environment. The increasing pH induces the formation of crystalline $CaHPO_4 \cdot mH_2O$, TCP or HAp to fill the dentinal tubule. The chemical reactions are suggested as follows:

$$Ca^{2+} + H_2PO_4^- \rightarrow CaHPO_4(DCPD) + H^+$$

$$Ca^{2+} + HPO_4^{2-} \rightarrow CaHPO_4$$

$$HPO_4^{2-} + H^+ \leftrightarrow H_2PO_4^-$$

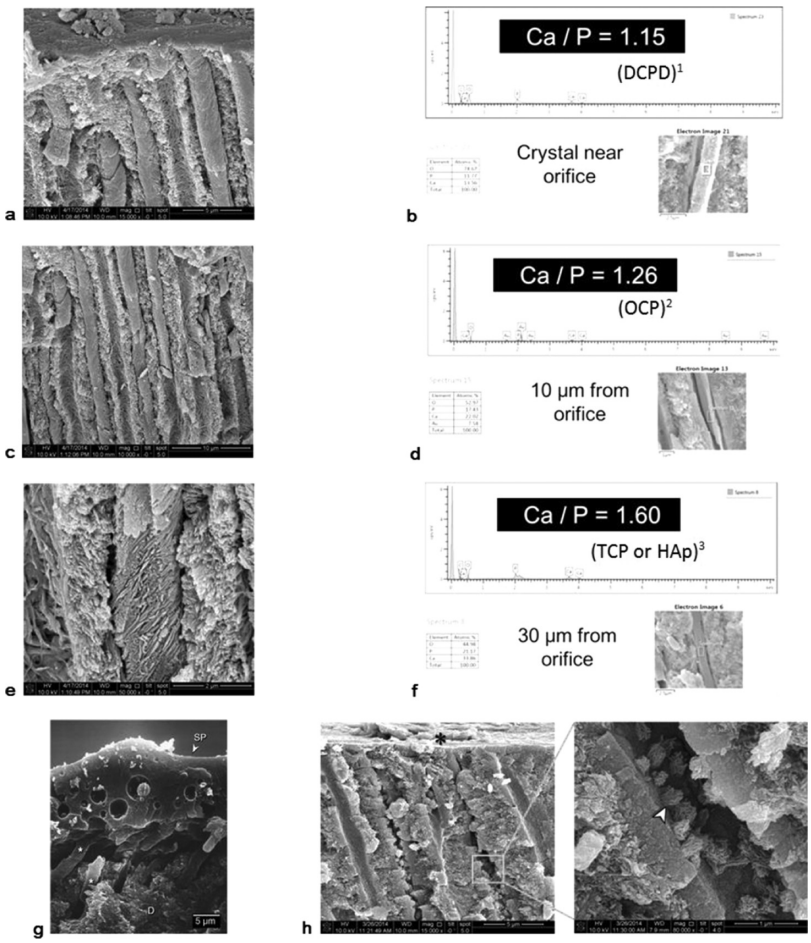

Figure 6. ***In vivo*** **precipitates of CCMS-HP in an animal model (12-month-old mongrel dog) with SEM/EDS evaluations. (a) Integrated crystals formed within dentinal tubules from the tooth cavity surface. (b) EDS identified the precipitate near the orifices of dentinal tubules as DCPD crystals (Ca/P = 1.15). (c) SEM showed occlusion of the dentinal tubules at depths of 5−15 μm. (d) The crystals formed at depths of 10 μm in the dentinal tubules are OCP-like (Ca/P = 1.26). (e) and (f) show that crystals formed at depths of 30−40 μm in the dentinal tubules appear to undergo HAp- or TCP-like crystallization (Ca/P = 1.60). (g) A tooth treated with a commercial product (control group), Seal & Protect (SP, arrowheads), had a resin layer thickness of 5−10 μm covering the dentin surface (D, dentin), and some short resin tags (asterisks) penetrated the dentinal tubules. A gap of approximately 10 μm was observed between Seal & Protect and the dentin surface. (h) Incomplete crystallization of CCMC-HP within some dentinal tubules was observed. *A tooth cavity surface with the CCMS-HP crystalline layer. The arrowhead indicates the crystalline particles. [1]DCPD, dicalcium phosphate dihydrate, $CaHPO_4 \cdot 2H_2O$, Ca/P = 1.0; [2]OCP, octacalcium phosphate, $Ca_8(HPO_4)_2(PO_4)_4 \cdot 5H_2O$, Ca/P = 1.33; [3]TCP, tricalcium phosphate, $Ca_3(PO4)_2$, Ca/P = 1.5; [4]HAp, hydroxyapatite, $Ca_{10}(PO_4)_6(OH)_2$, Ca/P = 1.67.**

Thus, as soon as DCPD precipitates, the hydrogen ion byproduct creates a mildly acidic environment in which $H_2PO_4^-$ and HPO_4^{2-} can react with H^+ ions to form a buffer solution. Subsequently, the increasing pH value would be favorable for the growth of crystals with a higher Ca/P ratio. That is, crystal growth tends to develop with OCP, TCP, or HAp-like crystal patterns; meanwhile, the alkaline environment and the formed stable biomimetic crystals would protect the dentinal tubule from acid erosion.

CONCLUSIONS

The exposure of dentinal tubules is a critical etiology in dentinal hypersensitivity, the pathogenesis of dental caries, and pulpal and periapical diseases. We successfully synthesized a novel $CaCO_3$@mesoporous silicate (CCMS) using a gelatin template. CCMS mixed with 30% phosphoric acid (CCMS-HP) can lead to $CaHPO_4$ or HAp-like crystal growth on microporous dentin structures and can effectively occlude dentinal tubules with biomimetic crystalline precipitates. Similar efficacy was observed in a live animal model. The CCMS-HP paste was also biocompatible, as indicated by the dental pulp cell response in both *in vitro* and animal models. We demonstrated that phosphate ions play a crucial role in biomimetic crystal growth in dentinal tubules for two reasons. First, phosphate ions cause the release of calcium ions from CCMS-HP, liberating these ions to permeate the dentinal tubule to form a Ca−P precipitate. Second, the phosphoric ions work as targeting moieties, continuously attracting calcium ions, causing them to permeate the dentinal tubules. Crystal growth in dentinal tubules leads to TCP or HAp-like crystal structures as the pH increases due to the

evolution of the environment as the crystal growth proceeds. The biomimetic crystal layer can serve as a more reliable barrier that protects the pulp tissue. In fact, this crystal layer may act as a promoter for the mineralization of the pulp-dentin complex by inducing the permeation of calcium ions. We believe that the novel mesoporous biomaterials presented here have great potential for serving as both a catalyst and as a carrier in the repair or regeneration of dental hard tissue.

METHODS

Preparation of $CaCO_3$@Mesoporous Silica (Denoted as CCMS). Gelatin (1.0 g), which was selected as the organic template, was added to distilled water (25.0 g) and stirred at 40 °C for 15 min. An acidified silicate solution with an approximate pH of 5.0 was prepared by combining a solution of sodium silicate (4.0 g) and distilled water (100 g) with sulfuric acid (2.0 M, 40 °C). After pouring the gelatin solution, a silicate-gelatin gel solution formed within a few minutes. The gel solution was hydrothermally treated at 100 °C for 24 h. After filtering, drying, and calcining at 600 °C, the mesoporous silica $CaCO_3$ carrier was produced. A CCMS biomaterial with a Ca/Si molar ratio of 1/1 was prepared using a simple impregnation procedure. Calcined mesoporous silica (0.5 g) was mixed with an aqueous solution of $CaCO_3$ (0.84 g) and oxalic acid (0.09 g) as the $CaCO_3$ precursor, and then the mixture was dried at 100 °C. The obtained powder was calcined at 200−400 °C in air to form the CCMS. The mesostructure was examined using a transmission electron microscope (TEM, Model H-7100, Hitachi, Tokyo, Japan).

***In Vitro* Efficacy of CCMS-HP in the Occlusion of Dentinal Tubules.** CCMS-HP was applied to 2 mm-thick dentin discs using a microbrush for 1 min, and the excess was wiped from the discs with wet cotton pellets. This step was repeated three times, and then the dentin surface was rinsed with water (pH 9). Treated dentin discs were stored for 24 h at 37 °C and 100% relative humidity. The dentin discs were produced by horizontally slicing intact human third molars. All human teeth used in this study were obtained from 16- to 40-year-old people from the National Taiwan University Hospital after appropriate informed written consent was provided. Prior to use, all teeth were stored at 4 °C in distilled water containing 0.2% thymol to inhibit microbial growth. To determine the optimal ratio of H_3PO_4 (85.7% phosphoric acid, J.T. Baker Analyzed, USA) and CCMS powder, CCMS-HP samples with Ca/P molar ratios of 2/1, 1/1, 1/2, 1/3, and 1/4 (CCMS (Ca) to 30% H_3PO_4 (P)) were prepared to evaluate the resulting pH values and crystal growth depths in dentinal tubules. The dentin disc specimens were split to examine the depth of crystallization in the dentinal tubules and the sealing quality in the dentinal tubules using field-emission scanning electron microscopy (FE-SEM, S-800, Hitachi, Tokyo, Japan). The crystalline phases resulting from the CCMS-HP paste (CCMS mixed with 30% H_3PO_4) were characterized using X-ray diffraction (XRD, Rigaku Denki Co., Ltd., Tokyo, Japan) with Cu Kα radiation and a Ni filter. The scan range was from 10° to 60° with a scan rate of 4°/min. The relative intensities of the characteristic peaks of each phase were used to determine the contents of the phases.

Sub-μ-CT (Sub-Micron Ultra-High Resolution X-ray Computed Tomography) Analysis. The samples were fixed and prepared as $1 \times 3 \times 3$ mm^3 pieces before sub-μ-CT scanning (Bruker Skyscan 1272, Kontich, Belgium). The scanning parameter was set as a voxel size of 500 nm^3 using a 60-keV voltage and 166 μA with a 1800 ms exposure time and a 0.25 mm aluminum filter in offset scanning conditions. Skyscan 1272 was set to acquire 1 photo per 0.1 degree. Certified calcium references (0.25 g/cm^3 and 0.75 g/cm^3) were scanned as the reference of Hounsfield Units under the same condition. Section reconstruction was performed using GPU-based scanner software (NRecon, Version 1.6.9.8, Bruker Skyscan). After reconstruction, the images were separated by Dataviewer software (Version 1.5.1, Bruker Skyscan), and the 3D images/videos were generated using CTVox software (Version 2.7, Bruker Skyscan). Region of interest (ROI) analyses were performed with CTAn (Version 1.13.10.1, Skyscan). Representative images and video were produced using CtVox (Version 2.7, Skyscan) to create volume rendering with surface lightning and shadows.

***In Vitro* Cytotoxicity Evaluation: WST-1 and Lactate Dehydrogenase (LDH) Assays.** The 3T3 fibroblast cell line was cultured in Dulbecco's Modified Eagle's Medium (DMEM) containing 10% fetal bovine calf serum (FBS) and 1% penicillin/streptomycin at 37 °C/5% CO_2. Cells at a culture passage of more than three were used. We evaluated the test materials using a transwell dentin disc model (TDD model, Supporting Information, Figure S5). The TDD model was established based on the modification of similar models used for numerous cytotoxicity studies.[29,45] The membrane insert of the transwell was replaced by a 200-μm-thick dentin disc from a healthy human tooth. We immersed the dentin discs in 17% EDTA, subjected the discs to ultrasonic vibration for 2 min to remove the smear layer, and thoroughly rinsed the discs with distilled water. The procedures used in subsequent experiments on different models were the same as those used for the transwell insert model. The transwells were transferred into 6-well culture plates (3.0 μm pore size, 24 mm in diameter; Transwell 3414, Costar, Corning, NY), which were seeded with 3T3 fibroblasts (2.5×10^4 cells/well) 24 h before the respective test materials were transferred to the transwells. The specimens were incubated at 37 °C/5% CO_2 for 24 and 72 h. After WST-1 staining and incubation, cell proliferation was evaluated by measuring the absorbance at 440 nm using an ELISA reader. Data were calculated as the ratio to the values obtained for untreated controls. The procedures of the LDH assay used for the experiments were the same as those for the WST-1 assay before the addition of LDH solution. After cell culturing for 24 and 72 h, 50 μL/well was transferred into a new 96-well plate. The residual medium was removed, and the cells coating the wells were frozen/killed at −80 °C. We added LDH solution (50 μL) to each well and stopped the reaction after 30 min using stop solution (50 μL/well). The absorbance was measured at 490 nm.

***In Vitro* Pulp Cell Response: Pulp Morphology and Alkaline Phosphatase (ALPase) Activity Assay.** We extracted healthy human teeth (third molars) after acquiring the appropriate informed written consent from donors. The freshly extracted teeth were immediately split to obtain pulp tissues, which were minced and cultured in DMEM containing 20% FBS with 1% penicillin/streptomycin. We cultured the cells at 37 °C/5% CO_2 and used cells at passages of 3−8. The pulp cells (1×10^4 cells/well) were seeded in 24-well culture plates for the elution model, and 2.5×10^4 cells/well were seeded for the TDD model 24 h before the respective materials were transferred to the transwells. Both groups of pulp cells exposed to the respective materials and the controls (DMEM and without the test material) were incubated for 5 d in a humidified CO_2 incubator at 37 °C. For ALP staining, cells were fixed with 4% paraformaldehyde for 20 min and stained with substrate solution (3 mg Naphthol AS phosphate (Sigma), 10 mg Fast Blue BB salt (Sigma), 0.05 mL *N*,*N*-dimethylformamide (Sigma) in 10 mL of 0.1 M Tris buffer [pH 9.1]) for 30 min. The morphologies and ALP staining of the pulp cells were examined using a light microscope (Olympus Co., Tokyo, Japan).

For the quantitative ALPase activity assay, after 5 days incubation, cells were lysed with 200 μL extraction buffer (0.1% Triton X-100 and 2 mM $MgCl_2$ in ddH_2O) for 15 min at 37 °C. ALPase activity in the lysates was measured in alkaline buffer solution (Sigma, A9226) with alkaline phosphate yellow liquid substrate (Sigma, P7998) for 30 min at 37 °C. Reactions were stopped by the addition of 3 M NaOH solution and absorbance of the reactions was read at 405 nm. The total protein quantitation was assayed using a bicinchoninic acid

(BCA) protein assay kit (Santa Cruz Biotechnologies, sc-202389), and ALPase activity was normalized to protein concentration (nmol/μg of protein/30 min).

For statistical analysis, all WST-1 and LDH data were analyzed using SPSS 16.0 statistical software (SPSS Inc., Chicago, IL, USA). Statistical comparisons were conducted using one-way ANOVA, followed by a *post hoc* Tukey test with the statistical significance set at $\alpha = 0.05$. An ALP activity assay was statistically analyzed using the Mann−Whitney U test.

Animal Study: Surgical Procedures. Mongrel dogs (12−15 months old, 10−12 kg) were used in the study. All animal experiments were performed under approval from the Research Review Board and Animal Ethical Committee, National Taiwan University. The dogs were anesthetized with an intramuscular injection of Tiletamine/Zolazepam (10 mg/kg, Zoletil; Virbac Lab., France) and Xylazine (5 mg/kg, Rompun, Bayer, Germany). Teeth cavities (5 mm in length, 3 mm in width, and 2 mm in depth) were prepared on the buccal surface of both the maxillary and mandibular canine and first molar. The exposed dentin cavity was subsequently etched with 37.5% phosphoric acid gel (Gel etchant, Kerr Co., CA, USA) for 10−15 s to remove the smear layer and to open the dentinal tubules to simulate the patent dentinal tubules. Each tooth was thoroughly washed with distilled water. Two test materials (Seal & Protect and CCMS-HP) and one control group (IRM, immediate restorative material, Dentsply Detrey) were used in the animal studies. Each test material was randomly assigned to 18 cavities ($n = 6$ for each time point, 7, 28, and 70 d).

Animal Study: *In Vivo* Efficacy, Pulp Irritation Assay and Crystal Characterization. Teeth were extracted 7, 28, and 70 days after treatment, in accordance with ISO-7405. We split the extracted teeth to determine whether the dentinal tubules were occluded. The depths and elemental compositions of the precipitates and the morphologies of the dentin substrates were examined using FE-SEM and EDS. For the dental pulp irritation tests, other parts of the split specimens were prepared for histological analysis using hematoxylin and eosin (H&E) stain. The intensity of the pulp response was evaluated using a light microscope. Pulp inflammation was categorized from "none" to "severe" according to the criteria proposed by Heyeraas *et al.*[42] The criteria are briefly described as follows: Score 0 (none), normal pulpal tissue; Score 1 (mild), a few inflammatory cells and a few extravasated red blood cells may be found; Score 2 (moderate), neutrophilic and mononuclear leukocytes may invade the odontoblast-predentin area (odontoblasts cannot be identified in their normal pseudostratified appearance); and Score 3 (severe), marked cellular infiltration, including abscess formation. Polymorphonuclear and mononuclear leukocytes were predominant in the affected area. The differences in dental pulp inflammation scores among the groups in each observation period were analyzed using the Kruskal−Wallis test with Dunn's post-test (the statistical significance was set at $\alpha = 0.05$). The Ca/P of the crystals grown in the dentinal tubules was investigated by a SEM/EDS examination (Hitachi S-2400; Nova NanoSEM 30 series, FEI, HK). The spot size of EDS was 1.8 nm and the penetration depth was 1.5 μm.

Conflict of Interest: The authors declare no competing financial interest.

Acknowledgment. This study was partly supported with funding from the National Science Council (97-2314-B-002-105) and the National Taiwan University Hospital (96-S653 &100-N1766).

Supporting Information Available: Mechanism of crystal growth within dentinal tubules, sub-μ-CT video, and elemental analysis are given in detail. This material is available free of charge *via* the Internet at http://pubs.acs.org.

REFERENCES AND NOTES

1. Vieira, A. R.; Siqueira, J. F., Jr.; Ricucci, D.; Lopes, W. S. Dentinal Tubule Infection as the Cause of Recurrent Disease and Late Endodontic Treatment Failure: A Case Report. *J. Endod.* **2012**, *38*, 250–254.
2. Bergamini, M. R.Bernardi, M. M.; Sufredini, I. B.; Ciaramicoli, M. T.Kodama, R. M.; Kabadayan, F.; Saraceni, C. H. Dentin Hypersensitivity Induces Anxiety and Increases Corticosterone Serum Levels in Rats. *Life Sci.* **2014**, *98*, 96–102.
3. Brannstrom, M. Dentin Sensitivity and Aspiration of Odontoblasts. *J. Am. Dent. Assoc., JADA* **1963**, *66*, 366–370.
4. Addy, M.; Embery, G.; Edgar, W. M.; Orchardson, R. *Tooth Wear and Sensitivity: Clinical Advances in Restorative Dentistry*; Martin Dunitz, Ltd.: London, U.K., 2000; pp 339−362.
5. Lin, P. Y.; Cheng, Y. W.; Chu, C. Y.; Chien, K. L.; Lin, C. P.; Tu, Y. K. In-Office Treatment for Dentin Hypersensitivity: A Systematic Review and Network Meta-Analysis. *J. Clin. Periodontol.* **2013**, *40*, 53–64.
6. West, N. X.; Lussi, A.; Seong, J.; Hellwig, E. Dentin Hypersensitivity: Pain Mechanisms and Aetiology of Exposed Cervical Dentin. *Clin. Oral Invest.* **2013**, *17* (Suppl 1), S9–19.
7. Absi, E. G.; Addy, M.; Adams, D. Dentine Hypersensitivity. A Study of the Patency of Dentinal Tubules in Sensitive and Non-Sensitive Cervical Dentine. *J. Clin. Periodontol.* **1987**, *14*, 280–284.
8. Pashley, D. H. Dentin-Predentin Complex and Its Permeability: Physiologic Overview. *J. Dent. Res.* **1985**, *64* (Spec No), 613–620.
9. Rusin, R. P.; Agee, K.; Suchko, M.; Pashley, D. H. Effect of a New Desensitizing Material on Human Dentin Permeability. *Dent. Mater.* **2010**, *26*, 600–607.
10. Kolker, J. L.; Vargas, M. A.; Armstrong, S. R.; Dawson, D. V. Effect of Desensitizing Agents on Dentin Permeability and Dentin Tubule Occlusion. *J. Adhes. Dent.* **2002**, *4*, 211–221.
11. Pashley, D. H.; Matthews, W. G.; Zhang, Y.; Johnson, M. Fluid Shifts across Human Dentine *in Vitro* in Response to Hydrodynamic Stimuli. *Arch. Oral Biol.* **1996**, *41*, 1065–1072.
12. Greenhill, J. D.; Pashley, D. H. The Effects of Desensitizing Agents on the Hydraulic Conductance of Human Dentin *in Vitro*. *J. Dent. Res.* **1981**, *60*, 686–698.
13. Suge, T.; Ishikawa, K.; Kawasaki, A.; Yoshiyama, M.; Asaoka, K.; Ebisu, S. Duration of Dentinal Tubule Occlusion Formed by Calcium Phosphate Precipitation Method: *In Vitro* Evaluation Using Synthetic Saliva. *J. Dent. Res.* **1995**, *74*, 1709–1714.
14. Clark, D. C.; Hanley, J. A.; Geoghegan, S.; Vinet, D. The Effectiveness of a Fluoride Varnish and a Desensitizing Toothpaste in Treating Dentinal Hypersensitivity. *J. Periodontal. Res.* **1985**, *20*, 212–219.
15. Schlueter, N.; Hardt, M.; Lussi, A.; Engelmann, F.; Klimek, J.; Ganss, C. Tin-Containing Fluoride Solutions as Anti-Erosive Agents in Enamel: An *in Vitro* Tin-Uptake, Tissue-Loss, and Scanning Electron Micrograph Study. *Eur. J. Oral Sci.* **2009**, *117*, 427–434.
16. Petrou, I.; Heu, R.; Stranick, M.; Lavender, S.; Zaidel, L.; Cummins, D.; Sullivan, R. J.; Hsueh, C.; Gimzewski, J. K. A Breakthrough Therapy for Dentin Hypersensitivity: How Dental Products Containing 8% Arginine and Calcium Carbonate Work to Deliver Effective Relief of Sensitive Teeth. *J. Clin. Dent.* **2009**, *20*, 23–31.
17. Ayad, F.; Ayad, N.; Zhang, Y. P.; DeVizio, W.; Cummins, D.; Mateo, L. R. Comparing the Efficacy in Reducing Dentin Hypersensitivity of a New Toothpaste Containing 8.0% Arginine, Calcium Carbonate, and 1450 ppm Fluoride to a Commercial Sensitive Toothpaste Containing 2% Potassium Ion: An Eight-Week Clinical Study on Canadian Adults. *J. Clin. Dent.* **2009**, *20*, 10–16.
18. Vahid Golpayegani, M.; Sohrabi, A.; Biria, M.; Ansari, G. Remineralization Effect of Topical Novamin *Versus* Sodium Fluoride (1.1%) on Caries-Like Lesions in Permanent Teeth. *J. Dent. (Tehran, Islamic Repub. Iran)* **2012**, *9*, 68–75.
19. Orchardson, R.; Gillam, D. G. Managing Dentin Hypersensitivity. *J. Am. Dent. Assoc., JADA* **2006**, *137*, 990–998.
20. Moritz, A.; Schoop, U.; Goharkhay, K.; Aoid, M.; Reichenbach, P.; Lothaller, M. A.; Wernisch, J.; Sperr, W. Long-Term Effects of Co2 Laser Irradiation on Treatment of Hypersensitive Dental Necks: Results of an *in Vivo* Study. *J. Clin. Laser Med. Surg.* **1998**, *16*, 211–215.

21. Thomas, H. F. The Lamina Limitans of Human Dentinal Tubules. *J. Dent. Res.* **1984**, *63*, 1064–1066.
22. Tanase, C. E.; Sartoris, A.; Popa, M. I.; Verestiuc, L.; Unger, R. E.; Kirkpatrick, C. J. *In Vitro* Evaluation of Biomimetic Chitosan-Calcium Phosphate Scaffolds with Potential Application in Bone Tissue Engineering. *Biomed. Mater.* **2013**, *8*, 1–10.
23. LeGeros, R. Z. Calcium Phosphates in Oral Biology and Medicine. *Monogr. Oral Sci.* **1991**, *15*, 1–201.
24. He, C.; Xiao, G.; Jin, X.; Sun, C.; Ma, P. X. Electrodeposition on Nanofibrous Polymer Scaffolds: Rapid Mineralization, Tunable Calcium Phosphate Composition and Topography. *Adv. Funct. Mater.* **2010**, *20*, 3568–3576.
25. Imai, Y.; Akimoto, T. New Method of Treatment for Dentin Hypersensitivity by Precipitation of Calcium Phosphate *in Situ*. *Dent. Mater. J.* **1990**, *9*, 167–172.
26. Ishikawa, K.; Eanes, E. D.; Tung, M. S. The Effect of Supersaturation on Apatite Crystal Formation in Aqueous Solutions at Physiologic Ph and Temperature. *J. Dent. Res.* **1994**, *73*, 1462–1469.
27. Lee, B. S.; Tsai, H. Y.; Tsai, Y. L.; Lan, W. H.; Lin, C. P. *In Vitro* Study of Dp-Bioglass Paste for Treatment of Dentin Hypersensitivity. *Dent. Mater. J.* **2005**, *24*, 562–569.
28. Lee, B. S.; Kang, S. H.; Wang, Y. L.; Lin, F. H.; Lin, C. P. *In Vitro* Study of Dentinal Tubule Occlusion with Sol-Gel Dp-Bioglass for Treatment of Dentin Hypersensitivity. *Dent. Mater. J.* **2007**, *26*, 52–61.
29. Kuo, T. C.; Lee, B. S.; Kang, S. H.; Lin, F. H.; Lin, C. P. Cytotoxicity of Dp-Bioglass Paste Used for Treatment of Dentin Hypersensitivity. *J. Endod.* **2007**, *33*, 451–454.
30. Wu, S. H.; Mou, C. Y.; Lin, H. P. Synthesis of Mesoporous Silica Nanoparticles. *Chem. Soc. Rev.* **2013**, *42*, 3862–3875.
31. Sakthivel, A.; Pedro, F. M.; Chiang, A. S.; Kuhn, F. E. Grafting of Cyclopentadienyl Ruthenium Complexes on Aminosilane Linker Modified Mesoporous Sba-15 Silicates. *Dalton Trans.* **2007**, 320–326.
32. Yeh, Y. Q.; Lin, H. P.; Tang, C. Y.; Mou, C. Y. Mesoporous Silica Sba-15 Sheet with Perpendicular Nanochannels. *J. Colloid Interface Sci.* **2011**, *362*, 354–366.
33. Sakthivel, A.; Huang, S. J.; Chen, W. H.; Lan, Z. H.; Chen, K. H.; Lin, H. P.; Mou, C. Y.; Liu, S. B. Direct Synthesis of Highly Stable Mesoporous Molecular Sievescontaining Zeolite Building Units. *Adv. Funct. Mater.* **2005**, *15*, 253–258.
34. Li, C. C.; Chen, Y. W.; Lin, R. J.; Chang, C. C.; Chen, K. H.; Lin, H. P.; Chen, L. C. A Self-Reductive Mesoporous CuO(X)/Fe/Silicate Nanocomposite as a Highly Active and Stable Catalyst for Methanol Reforming. *Chem. Commun. (Cambridge, U. K.)* **2011**, *47*, 9414–9416.
35. Chiang, Y. C.; Chen, H. J.; Liu, H. C.; Kang, S. H.; Lee, B. S.; Lin, F. H.; Lin, H. P.; Lin, C. P. A Novel Mesoporous Biomaterial for Treating Dentin Hypersensitivity. *J. Dent. Res.* **2010**, *89*, 236–240.
36. Hoppenbrouwers, P. M.; Driessens, F. C.; Borggreven, J. M. The Vulnerability of Unexposed Human Dental Roots to Demineralization. *J. Dent. Res.* **1986**, *65*, 955–958.
37. Featherstone, J. D.; Lussi, A. Understanding the Chemistry of Dental Erosion. *Monogr. Oral Sci.* **2006**, *20*, 66–76.
38. Damen, J. J.; Ten Cate, J. M. Silica-Induced Precipitation of Calcium Phosphate in the Presence of Inhibitors of Hydroxyapatite Formation. *J. Dent. Res.* **1992**, *71*, 453–457.
39. Li, P.; Nakanishi, K.; Kokubo, T.; de Groot, K. Induction and Morphology of Hydroxyapatite, Precipitated from Metastable Simulated Body Fluids on Sol-Gel Prepared Silica. *Biomaterials* **1993**, *14*, 963–968.
40. Damen, J. J.; ten Cate, J. M. The Effect of Silicic Acid on Calcium Phosphate Precipitation. *J. Dent. Res.* **1989**, *68*, 1355–1359.
41. Rashid, F.; Shiba, H.; Mizuno, N.; Mouri, Y.; Fujita, T.; Shinohara, H.; Ogawa, T.; Kawaguchi, H.; Kurihara, H. The Effect of Extracellular Calcium Ion on Gene Expression of Bone-Related Proteins in Human Pulp Cells. *J. Endod.* **2003**, *29*, 104–107.
42. Heyeraas, K. J.; Sveen, O. B.; Mjor, I. A. Pulp-Dentin Biology in Restorative Dentistry. Part 3: Pulpal Inflammation and Its Sequelae. *Quintessence Int.* **2001**, *32*, 611–625.
43. Gerzina, T. M.; Hume, W. R. Effect of Hydrostatic Pressure on the Diffusion of Monomers through Dentin *in Vitro*. *J. Dent. Res.* **1995**, *74*, 369–373.
44. Suge, T.; Ishikawa, K.; Kawasaki, A.; Suzuki, K.; Matsuo, T.; Noiri, Y.; Imazato, S.; Ebisu, S. Calcium Phosphate Precipitation Method for the Treatment of Dentin Hypersensitivity. *Am. J. Dent.* **2002**, *15*, 220–226.
45. Schmalz, G.; Schweikl, H. Characterization of an *in Vitro* Dentin Barrier Test Using a Standard Toxicant. *J. Endod.* **1994**, *20*, 592–594.